

# FLOW CALIBRATION OF TWO HYPERSONIC NOZZLES IN THE AEDC HEAT-H2 HIGH-ENTHALPY ARC-HEATED WIND TUNNEL\*

D. M. Smith\*\* and D. B. Carver  
Calspan Corporation/AEDC Operations  
Arnold Engineering Development Center  
Arnold Air Force Base, Tennessee 37389

19960913 178

## Abstract

The Arnold Engineering Development Center (AEDC) has added to its test facility inventory an arc-heated wind tunnel that can provide a large free-jet (up to 42-in. diam at the nozzle exit) hypersonic flow. The tunnel, designated HEAT-H2, uses air for true-temperature, true-pressure simulations at velocities up to 15,000 ft/sec and altitudes up to 165,000 ft. Existing conical nozzles yield flow Mach numbers from 4 to 8. Included herein is a summary of facility capabilities and selected results from an initial flow-field calibration. Two free-jet nozzles were calibrated, a 9-in.-exit diam nozzle and a 24-in.-exit diam nozzle, both with 1.5-in.-diam throats. Measurements within the free jet included distributions of pitot pressure, total enthalpy, and flow angle. Surface pressure and heat flux data on blunt cones and wedges were also obtained. Arc heater chamber conditions ranged from 31 to 65 atm pressure, with total enthalpy from 1,500 to 2,160 Btu/lbm. The facility should prove useful for a wide variety of hypersonic testing requirements including aerothermal testing of structures, heat shields, antenna windows, etc., and aeropropulsion testing of scramjet combustors.

## Nomenclature

ALPHA	Flow angle referenced to nozzle centerline, deg
DALPHA	Measured deviation of flow angle from conical theory, deg
GAMMA	Ratio of specific heats
$H_0$	Stagnation enthalpy, Btu/lbm
HOB	Total enthalpy of air exiting the nozzle, defined by an energy balance on the heater, Btu/lbm

HINF	Total enthalpy inferred from measured heat flux and pitot pressure, Btu/lbm
$H_w$	Enthalpy of air at the probe wall temperature, Btu/lbm
$M_\infty$	Free-stream centerline Mach number at nozzle exit
P	Blunt pressure cone surface pressure, atm
PCH	Arc heater plenum (chamber) pressure, atm
$P_0'$	Pitot pressure, atm
$P_{nose}$	Blunt cone stagnation pressure
$\dot{q}_0$	Heat flux, Btu/ft <sup>2</sup> -sec
$r_n$	Probe nose radius, in.
X	Axial distance on probe surface from stagnation point in the direction of the flow, in.
$X_0$	Distance along nozzle centerline from nozzle exit plane to probe tip, in.
Y	Lateral distance from nozzle centerline along wedge surface, in

## Introduction

The AEDC HEAT-H2 arc-heated tunnel became operational in 1990 and initial calibrations were obtained with one nozzle/throat combination (24-in.-diam exit/1.5-in.-diam throat) in 1991.<sup>1</sup> Since that time AEDC has obtained additional calibration data using two nozzle configurations, a 9-in.-diam exit and a 24-in.-diam exit, both with 1.5-in.-diam throats.

Calibration data were obtained on eighteen test runs over the period of September 1991 through March 1993. A summary of facility capabilities is pre-

\*The research reported herein was performed by the Arnold Engineering Development Center (AEDC), Air Force Materiel Command. Work and analysis for this research were done by personnel of Calspan Corporation/AEDC Operations, technical services contractor for the AEDC aerospace flight dynamics facilities. Further reproduction is authorized to satisfy needs of the U. S. Government.

\*\*Member, AIAA.

sented along with typical calibration data. Results consistently agree with predictions.

for the remaining ten runs. A 1.5-in.-diam throat was used for all runs.

## Test Facility

### Arc Heater

The AEDC HEAT-H2 test unit,<sup>1-3</sup> a continuous-flow, electric arc-heated testing facility, expands arc-heated air to a hypersonic free jet in the environment of an evacuated test cell (see Fig. 1). The test unit utilizes an N-4 Huels-type arc heater to heat high-pressure air which is expanded through a nozzle to hypersonic velocity in the test chamber and subsequently passed through the diffuser, air cooler, and ducting to an exhaustor plant. The arc heater consists of two coaxial tubular electrodes separated by a swirl chamber. Air injected into the swirl chamber is heated by the d-c arc and vortex-stabilized along the main axis of the heater, with further stabilization of the arc provided by electromagnetic spin coils located at either end of the heater. A rotary model positioning system with five positions can be programmed to inject test models at various axial stations, advance or retract axially at specified rates, and expose models to the flow for various intervals of time (Fig. 2). The test cell and model positioner can accommodate models up to 36 in. long, and weighing up to 150 lb.

### Nozzles

A three-section, water-cooled conical nozzle (Fig. 3) with an 8-deg half-angle is presently available for varying the free-jet conditions. Exit diameters of 9, 24, and 42 in. are available. These exit diameters, together with three throat diameters (1.0, 1.5, and 2.0 in.), provide a wide range of free-stream test conditions. The free-stream Mach number and maximum reservoir pressure for each configuration are shown in Table 1, and the range of test conditions in Table 2.

For the calibration series, the arc heater was configured with the 9-in. nozzle for eight runs, and with the 24-in. nozzle

## Test Articles

### Transient Calorimeters and Pressure Probes

Heat flux and pressure probes of various geometries were used to calibrate the flow field. Probe

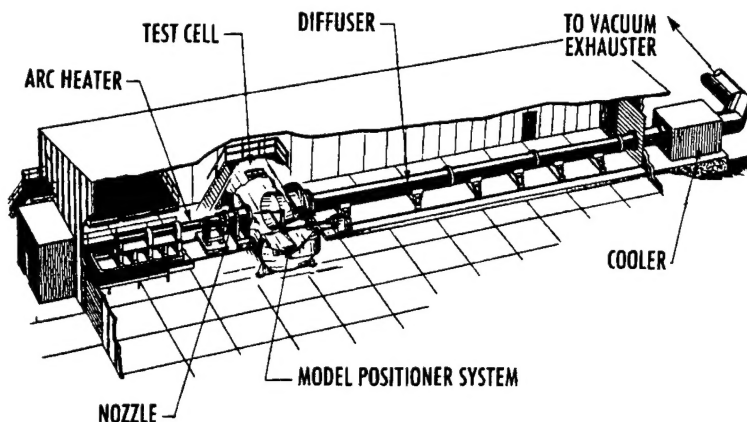


Fig. 1. HEAT-H2 arc-heated wind tunnel.

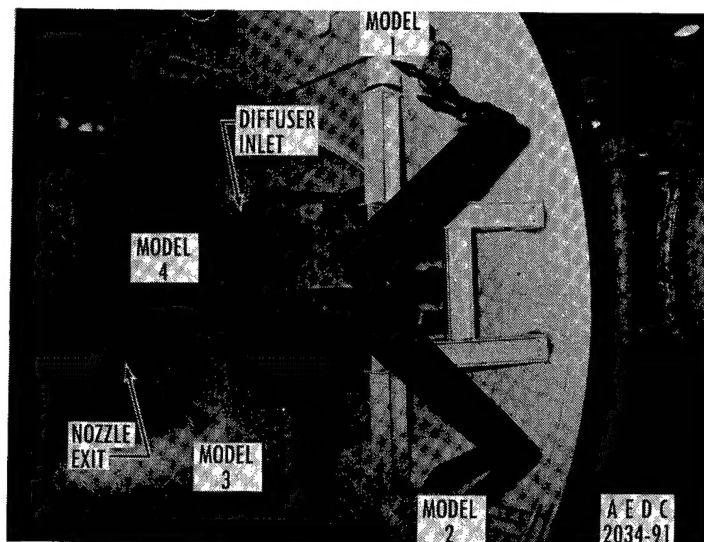


Fig. 2. Test cell and model positioner system.

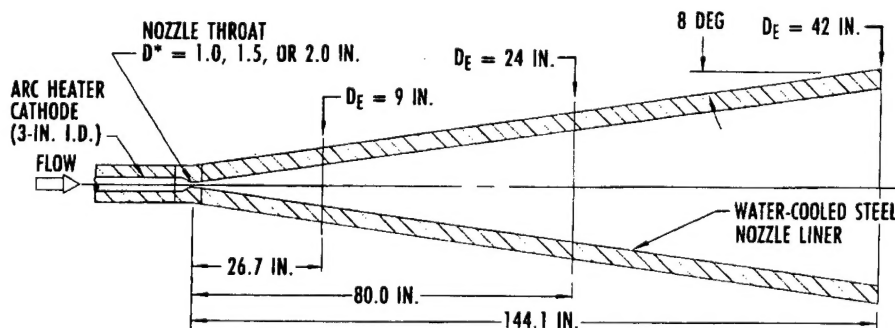


Fig. 3. HEAT-H2 8-deg conical nozzle configuration.

PLEASE CHECK THE APPROPRIATE BLOCK BELOW:

AO # M96-08-2026

☒ 1 copies <sup>is</sup> ~~are~~ being forwarded. Indicate whether Statement A, B, C, D, E, F, or X applies.

☒ DISTRIBUTION STATEMENT A:  
APPROVED FOR PUBLIC RELEASE: DISTRIBUTION IS UNLIMITED

☐ DISTRIBUTION STATEMENT B:  
DISTRIBUTION AUTHORIZED TO U.S. GOVERNMENT AGENCIES  
ONLY; (Indicate Reason and Date). OTHER REQUESTS FOR THIS  
DOCUMENT SHALL BE REFERRED TO (Indicate Controlling DoD Office).

☐ DISTRIBUTION STATEMENT C:  
DISTRIBUTION AUTHORIZED TO U.S. GOVERNMENT AGENCIES AND  
THEIR CONTRACTORS; (Indicate Reason and Date). OTHER REQUESTS  
FOR THIS DOCUMENT SHALL BE REFERRED TO (Indicate Controlling DoD Office).

☐ DISTRIBUTION STATEMENT D:  
DISTRIBUTION AUTHORIZED TO DoD AND U.S. DoD CONTRACTORS  
ONLY; (Indicate Reason and Date). OTHER REQUESTS SHALL BE REFERRED TO  
(Indicate Controlling DoD Office).

☐ DISTRIBUTION STATEMENT E:  
DISTRIBUTION AUTHORIZED TO DoD COMPONENTS ONLY; (Indicate  
Reason and Date). OTHER REQUESTS SHALL BE REFERRED TO (Indicate Controlling DoD Office).

☐ DISTRIBUTION STATEMENT F:  
FURTHER DISSEMINATION ONLY AS DIRECTED BY (Indicate Controlling DoD Office and Date) or HIGHER  
DoD AUTHORITY.

☐ DISTRIBUTION STATEMENT X:  
DISTRIBUTION AUTHORIZED TO U.S. GOVERNMENT AGENCIES  
AND PRIVATE INDIVIDUALS OR ENTERPRISES ELIGIBLE TO OBTAIN EXPORT-CONTROLLED  
TECHNICAL DATA IN ACCORDANCE WITH DoD DIRECTIVE 5230.25, WITHHOLDING OF  
UNCLASSIFIED TECHNICAL DATA FROM PUBLIC DISCLOSURE, 6 Nov 1984 (Indicate date of determination).  
CONTROLLING DoD OFFICE IS (Indicate Controlling DoD Office).

☐ This document was previously forwarded to DTIC on \_\_\_\_\_ (date) and the  
AD number is \_\_\_\_\_.

☐ In accordance with provisions of DoD instructions, the document requested is not supplied because:

☐ It will be published at a later date. (Enter approximate date, if known).

☐ Other. (Give Reason)

DoD Directive 5230.24, "Distribution Statements on Technical Documents," 18 Mar 87, contains seven distribution statements, as described briefly above. Technical Documents must be assigned distribution statements.

William M. Moss  
Authorized Signature/Date

William M. Moss  
Print or Type Name  
DSN 340-7329  
Telephone Number

Table 1. HEAT-H2 Nozzle Configurations

NOZZLE EXIT DIAMETER, IN.	THROAT DIAMETER, IN.	$M_{\infty}^*$	MAXIMUM TOTAL PRESSURE, ATM
9	1.0	5.3	100
	1.5	4.5	65
	2.0	4.0	35
24	1.0	7.8	100
	1.5	6.7	65
	2.0	5.9	35
42	1.0	8.3	100
	1.5	7.5	65

\* NOMINAL FREE-STREAM MACH NUMBER WAS CALCULATED ASSUMING AN EQUILIBRIUM AIR EXPANSION THROUGH THE NOZZLE AT MAXIMUM ENTHALPY AND PRESSURE CONDITIONS.

Table 2. HEAT-H2 Test Conditions

TOTAL ENTHALPY (BULK)	1,500 - 2,600 BTU/LBM
TOTAL TEMPERATURE	6,000 - 8,000°R
STATIC TEMPERATURE	500 - 2,500°R
AIR MASS FLOW RATE	2 - 10 LBM/SEC
TOTAL PRESSURE	300 - 1,500 PSIA (20 - 100 ATM)
STATIC PRESSURE	0.025 - 2 psia
MACH NUMBER	4 - 8
EQUIVALENT VELOCITY	10,000 - 15,000 FT/SEC
REYNOLDS NUMBER	$10^5$ - $10^6$ /FT
ALTITUDE	80 - 165 KFT
MODEL PITOT PRESSURE	2 - 50 PSIA
STAGNATION HEAT FLUX*	100 - 700 BTU/FT <sup>2</sup> -SEC

\* 1-IN NOSE RADIUS CALORIMETER, FLAT ENTHALPY MODE

geometry, instrumentation, and measured parameters for each probe are summarized in Table 3. Reference 1 includes details concerning the probes, instrumentation, and data reduction procedures.

### Procedure

### Test Conditions

Configured with the 1.5-in diam nozzle throat section, the H2 tunnel can provide a continuum of operating conditions with chamber pressures from 25 atm up to 65 atm. Arc heater power supply settings and air mass flow rate are matched to the chamber pressure selected, and can be changed, within limits, during the course of a single run. For the purposes of this calibration, two baseline operating conditions, 32- and 64-atm chamber pressure, were selected for ex-

Table 3. Calorimeters and Pressure Probes

DESCRIPTION	INSTRUMENTATION	MEASURED PARAMETER(S)
HEMISPHERE CALORIMETERS (0.25-IN. NOSE RADIUS)	NULL-POINT CALORIMETER (1) COAXIAL SURFACE THERMOCOUPLE (1)	STAGNATION HEAT FLUX
HEMISPHERE CALORIMETER (1.0-IN. NOSE RADIUS)	GARDON GAGES (2) NULL-POINT CALORIMETER (1)	STAGNATION HEAT FLUX 45 DEG HEAT FLUX
10/20 DEG CALIBRATION WEDGE (0.20-IN. NOSE RADIUS)	COAXIAL SURFACE THERMOCOUPLES (38) AND ELECTRONICALLY SCANNED PRESSURE (ESP) MODULE (29 ORIFICES)	WEDGE HEAT FLUX AND PRESSURE DISTRIBUTIONS
5-1/2 DEG CONE HEAT FLUX PROBE (0.25-IN. NOSE RADIUS)	COAXIAL SURFACE THERMOCOUPLES (11)	5-1/2 DEG CONE SURFACE HEAT FLUX
CYLINDRICAL LEADING EDGE CALORIMETER (1.0-IN. RADIUS)	GARDON GAGES (2) NULL-POINT CALORIMETER (1)	LEADING EDGE STAGNATION HEAT FLUX
PITOT PRESSURE PROBE	KULITE® STRAIN GAGE PRESSURE TRANSDUCER (1)	PITOT PRESSURE
7-EG BLUNT CONE PRESSURE PROBE	DRUCK® DIFFERENTIAL TRANSDUCER (1) ESP MODULE (27 ORIFICES)	PITOT PRESSURE CONE SURFACE PRESSURE
FLOW-ANGULARITY PROBE (WATER-COOLED)	DRUCK DIFFERENTIAL PRESSURE TRANSDUCERS (4)	FLOW ANGLE

tensive characterization. Calibration data were also obtained at intermediate chamber pressures. The baseline conditions selected provided bulk (energy balance) enthalpy levels generally between 1,500 and 2,200 Btu/lbm. Air mass flow rates were typically in the range from 5.2 to 9.8 lbm/sec, with total arc heater power in the range from 16 to 36 MW.

The air injection mode for the arc heater can be selected to provide a peaked enthalpy profile, with substantially higher centerline values, or a flat enthalpy profile, with a generally flat radial enthalpy profile. In order to provide heat flux and pressure distributions with maximum uniformity across the test jet, the arc heater was operated in the flat enthalpy air injection mode throughout the calibration series.

### Test Procedures

Conical nozzle flow is non-parallel, point-source flow, requiring systematic characterization of radial pressure and heat flux distributions at various axial positions inside the test free jet. The test conditions produced in a conical nozzle stream are characterized by parabolic radial pressure profiles, and static pressure which declines exponentially in the streamwise direction as a function of distance from the nozzle exit. Gas velocity (Mach number) increases in the streamwise direction as the flow expands in the free jet. Flow angle is a function of radial position in the free jet. A primary objective of this effort was to investigate conformity of measured flow parameters with calculations based on existing conical nozzle theory, in order to verify satisfactory operation of the various nozzle/throat combinations at high flow enthalpies and pressures.

The test procedure required stabilizing the arc heater at a selected operating condition, usually one of the two baseline conditions, then conducting a series of probe sweeps through the free jet at various axial positions to define conditions at the stagnation point and at gage locations on the various wedge and cone probe geometries. Flow calibration data for several operating conditions and/or flow axial positions were obtained in the course of a single run. A typical run provided from 30 to 40 individual probe sweeps. Each sweep provides a set of data points for each gage or transducer which defines the measured parameter across the entire test jet at the axial position and gage location of interest. Although probes were generally swept through the flow field, certain pressure measurements required a minimal dwell of the calibration probe at the flow field centerline. Dwell measurements were generally possible only with actively cooled probes.

### Data Reduction

Heat flux is calculated from the output of a null-point calorimeter or coaxial heat-transfer gage, using the temperature-time history of the gage thermocouple in a straight-forward solution of the heat conduction equations.<sup>4,5</sup> The local total enthalpy within the flow field is inferred from probe measurements of stagnation heat flux and pitot pressure, using the assumption of laminar flow on a hemisphere and an approximation to the Fay-Riddell relationship.<sup>6</sup>

$$\text{HINF} = [6.882 \dot{q}_0 / (p_0' / r_n)^{0.5}] + H_w, \text{ Btu/lbm} \quad (1)$$

### Calibration Results

#### Pitot Pressure and Enthalpy Profiles

Flow-field stagnation (or pitot) pressure profiles were measured with uncooled and water-cooled probes. Pitot pressure repeatability is shown in Fig. 4, with thirteen probe sweeps at a distance of 2 in. downstream of the 24-in. nozzle exit ( $X_0 = 2$ ). The profiles have been normalized by the measured arc heater chamber pressure, which ranged from 37-65 atm. The useful test core is seen to be at least 16 in. in diameter. A slight asymmetry is noted, with the pressure at the 6-in. radial position about 7 percent higher than the centerline pressure.

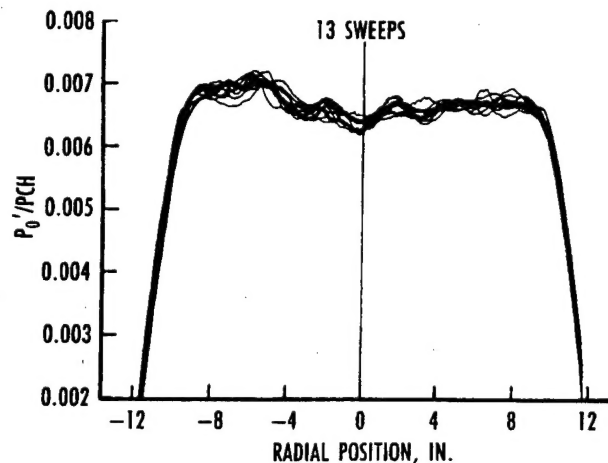


Fig. 4. Pitot pressure repeatability, 24-in. nozzle,  $X_0 = 2$ .

Averages of all pitot pressure profiles at several axial stations are shown in Figs. 5 and 6 for the 9-in. and 24-in. nozzles, respectively. These profiles show the expected axial pressure drop for a conical nozzle. Included on Fig. 5 are values predicted from a one-dimensional expansion of equilibrium air with a total enthalpy of 2,000 Btu/lbm.<sup>7</sup> Geometric area ratios were used for the theoretical values without any consideration for the boundary layer. An expansion wave emanates from the 9-in. nozzle exit, reducing



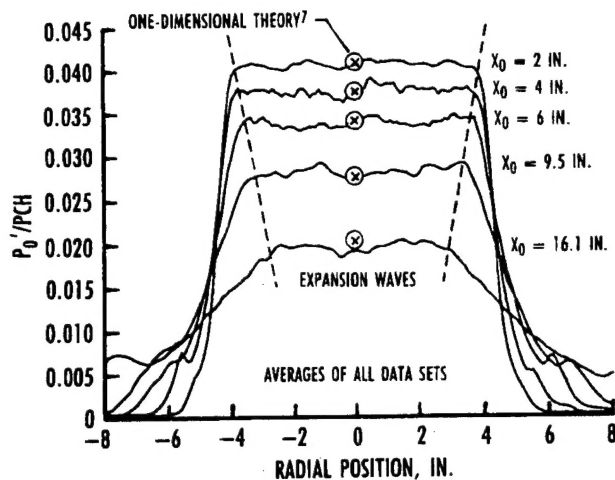


Fig. 5. Pitot pressure normalized to chamber pressure, 9-in. nozzle.

the effective core diameter from 8 in. (at  $X_0 = 2$  in.) to about 7 in. (at  $X_0 = 9.5$  in.). Profiles for the 24-in. nozzle exit (Fig. 6) do not exhibit either an expansion or compression wave, but the flow continues to expand. A useful test core of at least 16 in. diam is noted for all axial stations.

Enthalpy profiles inferred from the pitot pressure and stagnation heat flux measurements are shown in Figs. 7 and 8. Repeatability of the profiles as illustrated by Fig. 7 is generally better than  $\pm 10$  percent within the "core diameter" (6-in. core for 9-in. nozzle; 16-in. core for 24-in. nozzle). Temporal variations in the measured heat flux are the primary contributors to the sweep-to-sweep differences evident in Figs. 7 and 8. The swept probe technique requires fast responding sensors to prevent time-lag

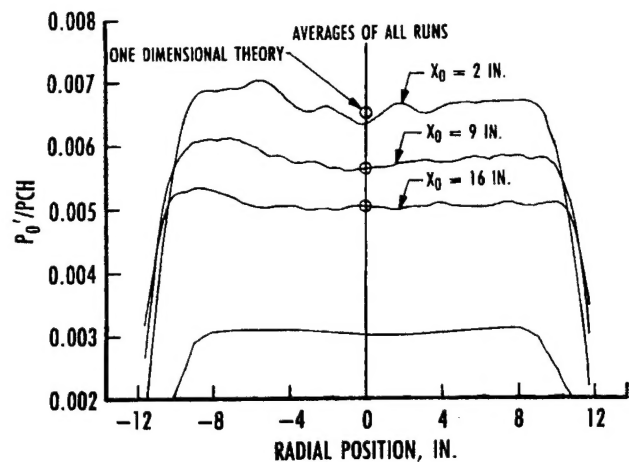
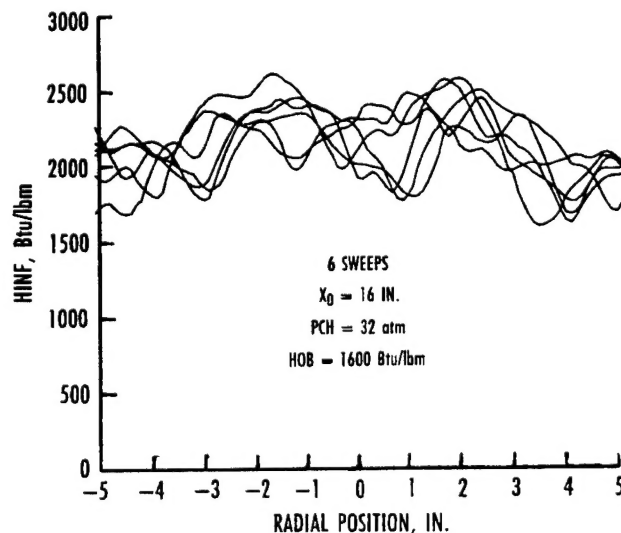
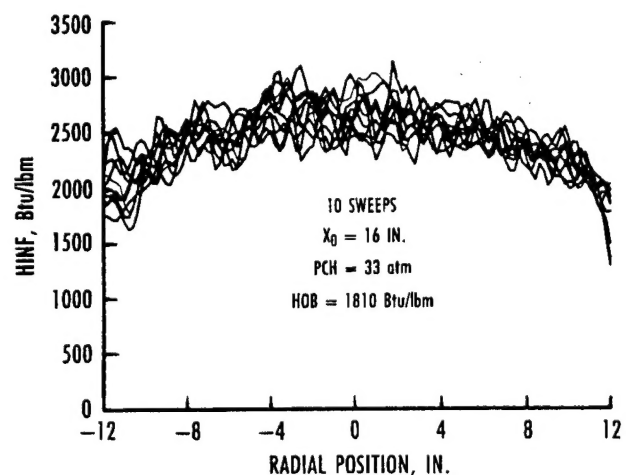


Fig. 6. Pitot pressure profiles at several axial position, 24-in. nozzle.

bias of the measurements. The sensors respond to arc heater condition variations and electromagnetic interference (EMI). For the present data it is estimated that at least half of the variation is a result of high-frequency ( $> 100$  Hz) fluctuations of energy input by the arc heater. The reader is referred to Ref. 8 for a discussion on heat-transfer measurement uncertainty in arc-heated flows. With enough sweeps (Fig. 7b), it becomes apparent that the spatial distribution of enthalpy is indeed fairly flat within the core diameter. Enthalpy profiles at three axial locations are shown in Fig. 8. The average profile of Fig. 8b indicates that the centerline enthalpy is about 10 percent higher than the core edge enthalpy (value 8 in. off centerline). Magnitudes within the core diameters are independent of axial location, but the  $X_0 = 2$  profiles drop off near the nozzle wall.

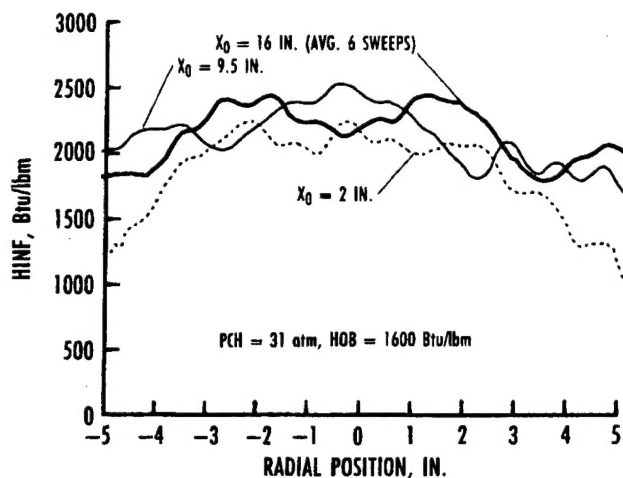


a. 9-in. nozzle

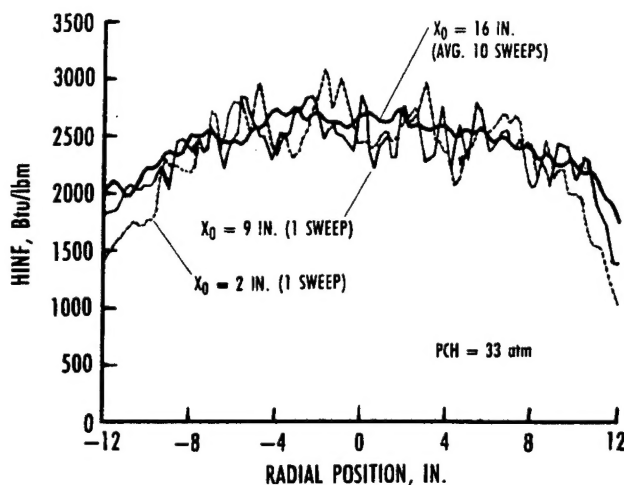


b. 24-in. nozzle

Fig. 7. Inferred enthalpy repeatability.



a. 9-in. nozzle



b. 24-in. nozzle

Fig. 8. Inferred enthalpy versus axial position.

In summary, the normalized pitot pressure profiles are independent of heater conditions over a wide range of chamber pressure and enthalpy. Local inferred enthalpy is nominally constant within the "core diameter," whereas pitot pressure decays axially, as expected for a conical nozzle. A properly designed contoured nozzle would therefore be expected to provide a uniform flow field both radially and axially, with maximum variations comparable to the radial variations of the present data.

### Flow Angularity Profiles

Inviscid cone pressure theory was used to define flow angles relative to the tip of flow angularity probe. Typical flow angularity profiles obtained for the 24-in. nozzle are presented in Fig. 9. Included in Fig. 9 are theoretical lines for conical (or source) flow. Maxi-

mum offset from theory is about 0.3 deg within the 16-in.-diam test core (Fig. 10).

### 7-deg Blunt Cone Pressures

A 7-deg half-angle blunt cone model was used to characterize the flow on the nozzle centerline. Data taken 2 in. from the nozzle exit are compared with conical flow theory in Fig. 11, showing that the trend definitely follows that of conical flow and the magnitude agrees with theory at a specific heat ratio ( $\gamma$ ) of 1.3. The data of Fig. 11 were obtained at three different test conditions, and the repeatability is generally better than  $\pm 2$  percent. The theoretical calculations were performed using a time-dependent flow-field simulation program (PARC Code).<sup>9</sup> The results shown were obtained using an inviscid option with constant specific heat ratios and a starting line computed from one-dimensional inviscid theory for source flow.

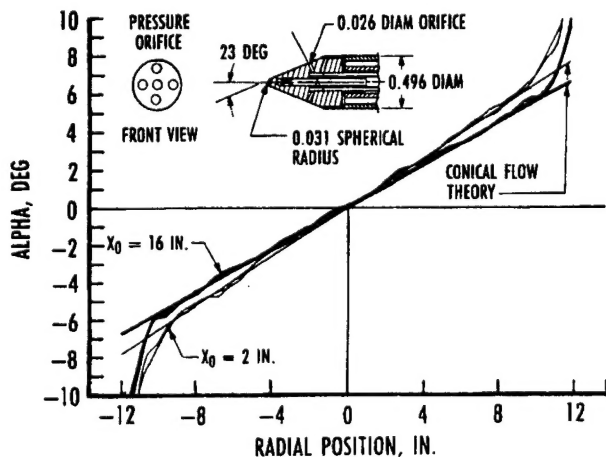


Fig. 9. Typical flow angularity profiles in the 24-in. nozzle.

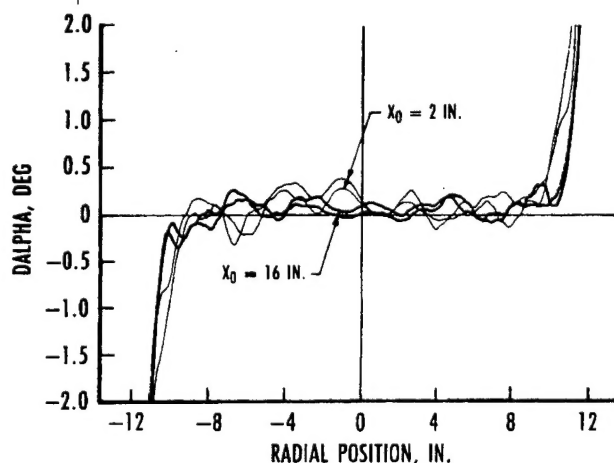


Fig. 10. Deviation from conical theory.

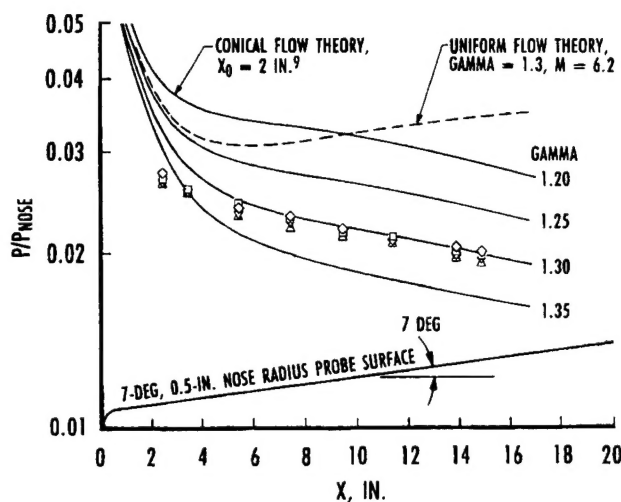


Fig. 11. Comparison of 7-deg cone data with conical flow theory.

### 10-deg and 20-deg Wedge Heat Flux Data

Wedge data were obtained as the model swept through the free jet, and during minimal dwells on the nozzle centerline. In all cases the data presented herein correspond to the wedge leading edge centered on the nozzle centerline (leading edge radial position equal to 0). Because the free-stream Reynolds number in the 9-in. nozzle is 2 to 10 times greater than in the 24-in. nozzle, it was expected that the flow could be tripped to produce turbulent heating levels. Some 9-in. nozzle data were obtained using trips (0.03-in. deep grooves) located immediately behind the wedge leading edge.

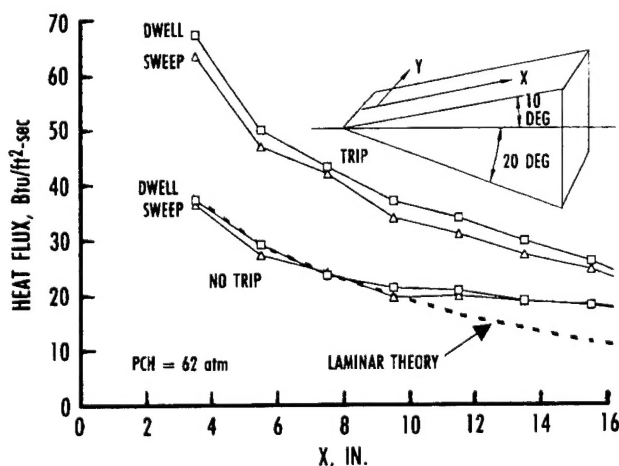


Fig. 12. Effect of boundary-layer trip on 10-deg wedge heat flux, 9-in. nozzle.

Longitudinal centerline heat flux distributions, with and without boundary-layer trips, on the 10-deg wedge in the 9-in. nozzle are shown in Fig. 12. The sweep and dwell data sets are in good agreement for all cases. "No trip" data are consistent with the laminar theory<sup>10</sup> near the leading edge, and it appears that

natural transition begins at about  $X = 10$  in. on the wedge.

The influence of wedge location relative to the nozzle ( $X_0$ ) is shown in Fig. 13 for the 9-in. nozzle and in Fig. 14 for the 24-in. nozzle. The levels generally decrease with increasing  $X_0$ , consistent with the lower pressure that was measured on the wedge surface, as would be expected in a conical nozzle.

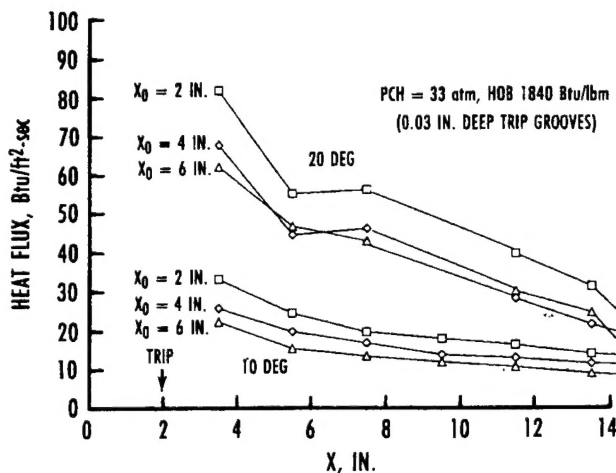


Fig. 13. Longitudinal centerline heat flux distributions on 10- and 20-deg wedges with trips, 9-in. nozzle.

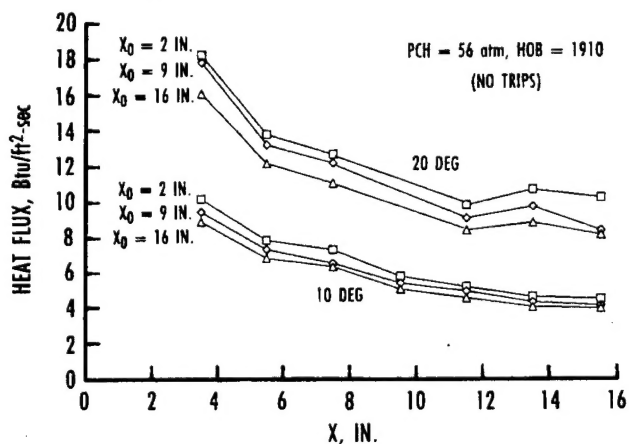


Fig. 14. Longitudinal centerline heat flux distributions on 10- and 20-deg wedges without trips, 24-in. nozzle.

Uniformity of lateral heat flux distributions on the 10-deg wedge, with trips, is shown in Fig. 15. The distribution at  $X = 5.5$  in. is very flat out to 3 in. either side of centerline, whereas at  $X = 15.5$  the flat region is limited to  $Y = \pm 1$  in.

### HEAT-H2 Flight Simulation Envelope

#### General

As illustrated in Fig. 16, HEAT-H2 in its various configurations provides ground test simulation



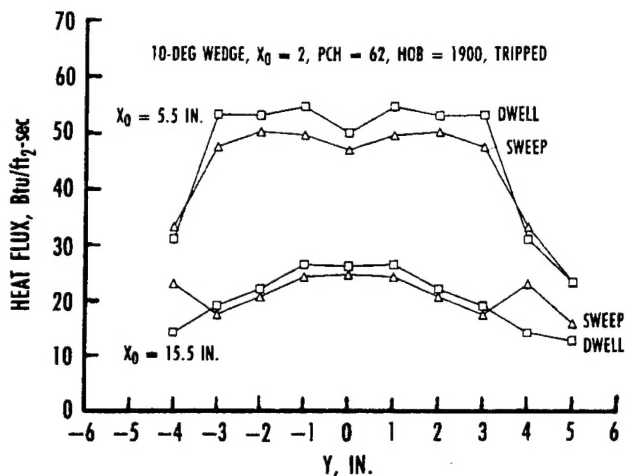


Fig. 15. Lateral distributions of turbulent heat flux at two axial stations, 9-in. nozzle.

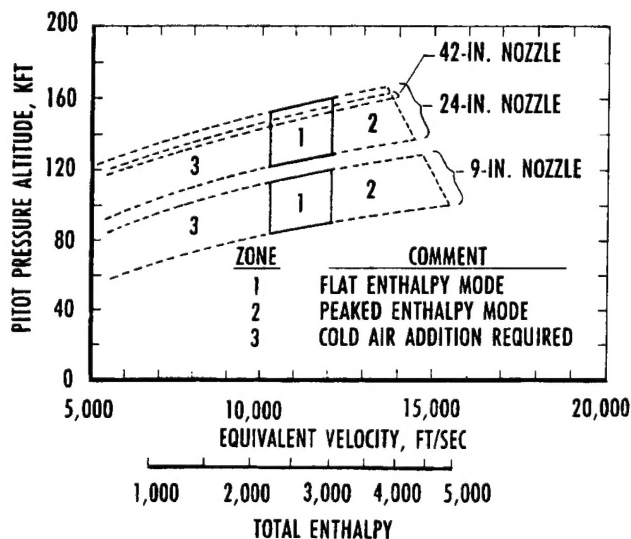


Fig. 16. Estimated HEAT-H2 free-jet test envelope.

capability from 80- to 165-kft pressure altitude, with enthalpy equivalent to flight at 10,000 to 15,000 ft/sec. The 9-in. nozzle configuration generally pro-

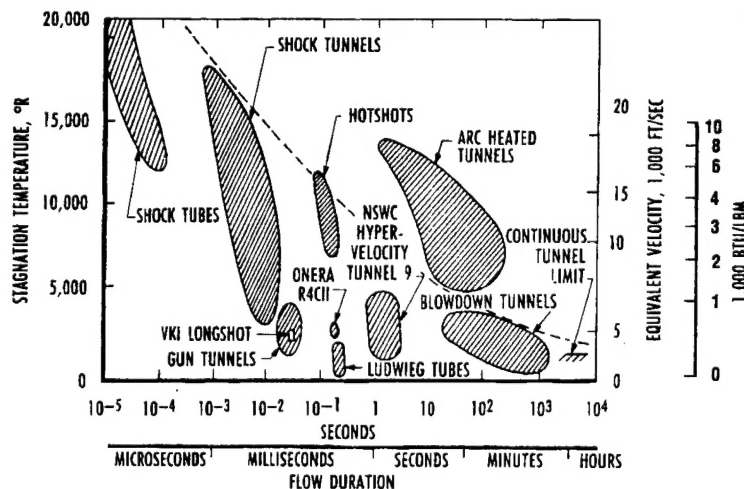


Fig. 17. High-temperature tunnel capabilities.

vides pitot pressure altitude simulations from 70 to 120 kft and velocity simulations to 15,000 ft/sec. The 24-in. nozzle can provide altitude simulations from 120 to 165 kft and velocity simulations to 14,000 ft/sec. The addition of cold mixing air capability for the heater, a possible future facility upgrade, would provide additional simulation capability down to 50-kft altitude and 6,000 ft/sec. Total enthalpy range on the nozzle centerline as now configured is 2,200 to 4,500 Btu/lbm.

The HEAT-H2 offers a unique range of test opportunities. Particularly suited for thermal structures testing, the tunnel is large enough to accommodate flight vehicle components in addition to basic material samples for evaluations at high-altitude, hypersonic flight conditions. The facility is suitable for antenna window/EM transmission studies, and is also capable of providing a scramjet combustor capability using the arc heater in a direct-connect mode to simulate flight velocities up to 11,000 ft/sec. Concept studies for a scramjet combustor test have been completed along with actual design and testing of critical components.<sup>11</sup>

### Exposure Times

Recent emphasis on the development of hypersonic flight vehicles makes arc-heated tunnels a natural choice for ground test simulation. This is particularly evident when long test times are necessary. Illustrated in Fig. 17 are various types of high-temperature tunnels shown as a function of flow duration. Only arc-heated tunnels can provide temperatures equivalent to velocities greater than 10,000 ft/sec for run times of more than 1 sec. Test times for the calibrations documented herein generally ranged from 2-5 min.

A transformer temperature limit presently restricts run times, depending on the arc heater amperage. Although not demonstrated to date, it should be possible to run for 10 min or longer at reduced amperage test conditions.

### Concluding Remarks

1. The HEAT-H2 was calibrated over a range of test conditions using a 1.5-in.-diam throat and conical free jet nozzles of 9-in. and 24-in. exit diam. The arc heater was configured to produce a "flat" enthalpy profile. Arc heater chamber conditions ranged from 31 to 65 atm, with total bulk enthalpies of 1,500 to 2,160 Btu/lbm.

2. Profiles of pitot pressure, flow angle, and total inferred enthalpy were used to define the free-jet test core. Useful test core diameters of 6 in. and 16 in. were demonstrated for the 9-in. and 24-in. exit diam nozzles, respectively.

3. All measurements correlate with theory for a conical-type nozzle with source flow.

4. HEAT-H2 is capable of providing true-temperature hypersonic flight simulations using air for test times up to 10 min.

5. Simulation scenarios include thermal structures, scramjet combustors, heat shields, and antenna windows (IR/RF).

### Acknowledgments

This work was funded by the Directorate of Aerospace Flight Dynamics Test (DOF), Arnold Engineering Development Center, Air Force Materiel Command. The AEDC program managers were Capt Brian Anderson and Lt Scott Tennent of the Facility Operations and Maintenance Division (DOFO).

Complete analysis and documentation of data from the calibration effort reported herein is currently in progress. A final report will be completed and published by December 1993. For more information on HEAT-H2, or to request a copy of the final data report, contact: AEDC/DOFO, Arnold AFB, TN 37389-4000.

### References

1. Davis, L. M. and Carver, D. B. "Initial Calibration of the HEAT-H2 Arc-Heated Wind Tunnel." AEDC-TR-91-16(AD-A245072), January 1992.

2. Felderman, E. J. et al. "AEDC Expanded Flow Arc Facility (HEAT-H2) Description and Calibration." ISA Paper 92-0191. Proceedings of 38th International Symposium, Las Vegas, NV, April 26-30, 1992.

3. MacDermott, W. N., Horn, D. D., and Fisher, C. J. "Flow Contamination and Flow Quality in Arc Heaters Used for Hypersonic Testing." AIAA-92-4028, AIAA 17th Aerospace Ground Testing Conference, Nashville, TN, July 6-8, 1992.

4. "Standard Method for Measuring Extreme Heat-Transfer Rates from High-Energy Environments Using a Transient, Null-Point Calorimeter." ASTM E-598-77, 1977 (Reapproved 1985).

5. Cook, J. W., and Felderman, E. J. "Reduction of Data From Thin-Film Heat-Transfer Gages: A Concise Numerical Technique." AIAA Journal Vol. 4, No. 3, March 1966.

6. Fay, J. A., and Riddell, F. R. "Theory of Stagnation Point Heat Transfer in Dissociated Air." Journal of the Aerospace Sciences, Vol. 25, No. 73, February 1958.

7. Jorgensen, L. H., and Baum, G. M. "Charts for Equilibrium Flow Properties of Air in Hypervelocity Nozzles." NASA TN D-1333, September 1962.

8. Carver, D. B., and Kidd, C. T. "Heat-Transfer Measurement Uncertainty Arc-Heated Flows." ISA Paper 91-115. Proceedings of the 37th International Instrumentation Symposium, San Diego, CA, May 5-9, 1991.

9. Cooper, G. K. and Sirbaugh, J. R. "PARC Distinction: A Practical Flow Simulator." AIAA-90-2002, June 1990.

10. Harms, Richard J., et al. "A Manual for Determining Aerodynamic Heating of High-speed Aircraft". Bell Aircraft Corp., Report No. 7006-3352-001, June 1959.

11. Stewart, J. H. "AEDC H2 Facility - New Capabilities for Hypersonic Air-Breathing Vehicles." AIAA-93-2781, July 1993.